AEM Journals.ASM.org

Acinetobacter Insertion Sequence IS*Aba11* Belongs to a Novel Family That Encodes Transposases with a Signature HHEK Motif

Barbara Rieck,[a] David S. Tourigny,[a] Marialuisa Crosatti,[a] Ralf Schmid,[b] Mandira Kochar,[a]* Ewan M. Harrison,[a] Hong-Yu Ou,[e] Jane F. Turton,[d] and Kumar Rajakumar[a,c]

Departments of Infection, Immunity and Inflammation[a] and Biochemistry,[b] University of Leicester, Leicester, United Kingdom; Department of Clinical Microbiology, University Hospitals of Leicester National Health Service Trust, Leicester, United Kingdom[c]; Health Protection Agency, Microbiology Services—Colindale, London, United Kingdom[d]; and Laboratory of Microbial Metabolism and School of Life Sciences and Biotechnology, Shanghai Jiaotong University, Shanghai, People's Republic of China[e]

Experimental and *in silico* PCR analysis targeting IS*Aba11* and Tn*AbaR* islands in 196 epidemiologically unrelated *Acinetobacter* strains representative of ≥19 species were performed. The first two *Acinetobacter baumannii* IS*Aba11* elements identified had been found to map to the same site on Tn*AbaR* transposons. However, no further evidence of physical linkage between the two elements was demonstrated. Indeed, examination of 25 definite or putative insertion sites suggested limited sequence specificity. Importantly, an *aacC1*-tagged version of IS*Aba11* was shown to actively transpose in *A. baumannii*. Similarity searches identified nine iso-IS*Aba11* elements in *Acinetobacter* and one in *Enhydrobacter* and single representatives of four distant homologs in bacteria belonging to the phyla "*Cyanobacteria*" and *Proteobacteria*. Phylogenetic, sequence, and structural analyses of IS*Aba11* and/or its associated transposase ($Tnp_{IS\mathit{Aba11}}$) suggested that these elements be assigned to a new family. All five homologs encode transposases with a shared extended signature comprising 16 invariant residues within the N2, N3, and C1 regions, four of which constituted the cardinal IS*Aba11* family HHEK motif that is substituted for the YREK DNA binding motif conserved in the IS*4* family. Additionally, IS*Aba11* family members were associated with either no flanking direct repeat (DR) or an IS*Aba11*-typical 5-bp DR and possessed variable-length terminal inverted repeats that exhibited extensive intrafamily sequence identity. Given the limited pairwise identity among $Tnp_{IS\mathit{Aba11}}$ homologs and the observed restricted distribution of IS*Aba11*, we propose that substantial gaps persist in the evolutionary record of IS*Aba11* and that this element represents a recent though potentially highly significant entrant into the *A. baumannii* gene pool.

Insertion sequences (IS) are small, typically <2.5-kb, self-transposable genetic elements present in all domains of life. More than 3,145 distinct IS elements have been identified in bacteria (http://www-is.biotoul.fr/), but only a minority have been demonstrated to actively transpose (13). Many IS families have been shown to be disseminated widely among multiple bacterial families, genera, and/or species (29).

Individual IS elements can be grouped into IS families based on characteristics such as transposase homology, transposase motifs, terminal inverted repeat (TIR) length, and composition, target specificity, and direct repeat (DR) length (6, 13). The majority of IS elements are flanked by DR sequences that arise from staggered DNA cuts at the target site, followed by pasting of the IS elements into the insertion locus. The highly dominant IS*4* family consists of members distributed throughout numerous organisms belonging to at least eight bacterial phyla and one archaeal phylum (6). In 2008, this large and broad IS*4* family was divided into seven recognizable subgroups. Additionally, 74 IS elements with variant forms of a transposase motif conserved in the IS*4* family were reclassified into three distinct novel IS families (6).

Only a few IS*4* family elements have been experimentally demonstrated to actively transpose *in vivo*. These include IS*231A* in *Bacillus thuringiensis* (9), IS*4Bsu1* in *Bacillus subtilis* (18) and IS*Aba1* in *Acinetobacter baumannii* (16). However, molecular mechanisms of transposition have been extensively studied for Tn*5* (26) and Tn*10* (10), both of which are resistance-encoding composite transposons with a central fragment and flanking terminal IS*4* family elements. In addition, crystal structures have been resolved for the Tn*5* transposase (Tnp_{Tn5}) (4). Tn*5* transposition is achieved by binding of transposase monomers to the target site, followed by transposase dimerization to form a highly ordered protein-DNA structure. Symmetrical contact of the left and right Tn*5* TIRs with both molecules of this dimer results in transposition (4).

The *A. baumannii* IS*Aba11* element encodes a predicted transposase that is identical to a hypothetical protein encoded by *A. baumannii* ATCC 17978 (31). The wider associated ATCC 17978 DNA sequence was subsequently recognized to constitute an insertion sequence designated IS*Aba11* and deposited in ISfinder (30) as a member of the IS*701* family (http://www-is.biotoul.fr/is.html). A. Rose, working in our laboratory, identified an identical IS element in *A. baumannii* strain A473 (27). His analysis revealed that IS*Aba11* contained matching 13-bp TIRs and was flanked by identical, target site-generated, 5-bp DRs (27). Remarkably, both of these IS*Aba11* elements had been found to be located in a location with the same sequence and in the same orientation within the *orf1* gene of Tn*AbaR* resistance islands. The *orf1* gene is the first of five predicted, tandemly orientated, transposition-associated

Received 1 June 2011 **Accepted** 2 November 2011
Published ahead of print 11 November 2011
Address correspondence to Kumar Rajakumar, kr46@le.ac.uk.
* Present address: Centre for Mycorrhizal Research, Biotechnology and Management of Bioresources Division, The Energy and Resources Institute, New Delhi, India.
Supplemental material for this article may be found at http://aem.asm.org/.

doi:10.1128/AEM.05663-11

genes in these Tn*7*-related transposons (27). The ~86-kb Tn*AbaR1* transposon, commonly designated the AbaR1 island, was first identified in *A. baumannii* strain AYE and found to carry 45 putative resistance genes (8). Subsequently, 18 other elements with features similar to those of Tn*AbaR1* were reported (12), although unlike counterparts in strains ATCC 17978 and A473, none carried IS*Aba11* elements. Most recently, Moffatt et al. (15) reported the presence and transposition of IS*Aba11* in *A. baumannii* ATCC 19606 and demonstrated a role for this element in the acquisition of colistin resistance through interruption of particular lipid A biosynthesis-associated genes (15).

The *Acinetobacter* genus comprises over 30 species. *A. baumannii* is the major human pathogenic species and accounts for an increasing burden of hospital-associated infections frequently caused by multiantibiotic-resistant clones circulating in hospitals worldwide (7). As of October 2011, 37 distinct IS elements had been identified in this genus (http://www-is.biotoul.fr/). Importantly, eight of these IS elements, IS*Aba1*, IS*Aba2*, IS*18*, an IS*3*-like element, IS*Aba3*, IS*Aba125*, IS*Aba825*, and IS*Aba11*, have been shown in *A. baumannii* to be associated with enhanced resistance to penicillins, cephalosporins, carbapenems, and colistin in natural clinical isolates and/or experimentally derived strains (15, 17, 23, 24).

In this study, we examined the distribution of IS*Aba11* within the *Acinetobacter* genus and demonstrated that this element actively transposes in *A. baumannii*. Sequence analysis and modeling of the IS*Aba11* transposase supported the hypothesis that IS*Aba11* belongs to a novel family that has diverged from the much broader and highly successful IS*4* superfamily.

MATERIALS AND METHODS

Bacterial strains, plasmids, genome sequences, and growth media. Details of the bacterial strains, plasmids, and genome sequences used in this study are listed in Tables S1 to S3 in the supplemental material. All strains were grown at 37°C in Luria-Bertani (LB) medium. *A. baumannii* colonies were selected following conjugation on Simmons citrate agar (Oxoid) supplemented with 80 μg/ml gentamicin.

DNA procedures. *Acinetobacter* DNA was isolated using the GenElute Bacterial Genomic DNA kit (Sigma) or the ArchivePure DNA Cell/Tissue and Tissue kit (5 Prime), while plasmid DNA was isolated using E.Z.N.A. Plasmid Miniprep Kit I (Omega Bio-Tec). Restriction enzymes (New England BioLabs) and T4 DNA ligase (Promega) were used as indicated by the suppliers, and chemical transformation and electrotransformation performed as previously described (28). For colony PCR, a single bacterial colony was resuspended in 30 μl of ultrapure water, heated at 94°C for 5 min, and centrifuged, and 2 μl of supernatant was used as the template. PCR assays were performed with GoTaq DNA polymerase (Promega) according to the manufacturer's instructions, except that dimethyl sulfoxide was added to a final concentration of 5%. The temperature cycling protocol used was 25 cycles of 95°C for 30 s, the annealing temperature for 30 s, and 72°C for 30 s; the annealing temperature was set at the melting temperature (T_m) minus 1°C for the primer with the lower of the two T_ms. Genomic walking was achieved by a two-step gene walking method (21). Finnzymes Phire Hot Start DNA polymerase (Fisher) was used with annealing performed at ≥60°C at a T_m as calculated at https://www.finnzymes.fi/tm_determination.html. Alternatively, inverse-PCR analysis was performed with outwardly facing IS*Aba11* primers and genomic DNA that had been first restricted and then religated to form single restriction fragment circular template molecules (19). Amplicons were purified using the E.Z.N.A. Cycle Pure kit (Omega Bio-Tec) and sequenced by Eurofins MWG Operon or GATC Biotech. For Southern blotting, 1 μg EcoRI-digested genomic DNA was resolved by agarose gel (0.8%) electrophoresis and capillary blotted onto positively charged nylon membrane (Bio-Rad). Hybridization and detection were performed as specified by the digoxigenin (DIG) High Prime DNA Labeling and Detection Starter kit (Roche).

Construction of a suicide vector carrying a tagged version of IS*Aba11*. An ~1.8-kb fragment containing an intact IS*Aba11* element was amplified from *A. baumannii* A473 DNA with primers orf1-F/orf1-R and cloned into pGEM-T Easy (Promega) to generate pISAba11. Next, a BamHI restriction site was introduced between the inverted repeat right (IRR) and the 3′ terminus of $tnp_{ISAba11}$ by inverse PCR with primers ISAba11-InF/ISAba11-InR. A 1,052-bp *aacC1* cassette from pUC18R6KminiTn7T-Gm was amplified with primers Gm-F-BamHI/Gm-R-BamHI and inserted into this BamHI site to generate pISAba11Gm. The 2.9-kb SacI/SphI *aacC1*-tagged IS*Aba11* fragment of pISAba11Gm was then ligated into the same sites in pDS132 (see Table S1 in the supplemental material) to construct pDSISAba11Gm. For details of the primers used in this study, see Table S4 in the supplemental material.

Bacterial conjugation. Overnight cultures of the donor strain KR1459 (*Escherichia coli* S17.1 λ *pir*/pDSISAba11Gm) and the *A. baumannii* A424 recipient strain were used to inoculate fresh LB medium that was then cultured to an optical density at 600 nm of 0.3 to 0.4. Equal volumes of exponential cultures of the donor and recipient strains were mixed and centrifuged at 16,000 × *g* (Sigma 1-14 microcentrifuge). Pellets were resuspended in 10% glycerol and spread onto LB agar plates, which were incubated at 37°C for overnight mating. The following day, bacteria were recovered by scraping and resuspended in 10% glycerol prior to plating of suitable dilutions onto Simmons citrate agar (Oxoid) supplemented with gentamicin (80 μg/ml). Plates were incubated at 37°C until colonies appeared.

Homology modeling. To compare structural features between the transposases of Tn*5* and IS*Aba11*, a homology model was built using Modeler (14). HHPred (32) and InterProScan (25) were used to identify and confirm Tnp_{Tn5} structures (HHPred E value for Protein Data Bank [PDB] entry 1MUS [33], 9.1e-22) as suitable templates for modeling of $Tnp_{ISAba11}$ and to provide a starting point for the target template alignment. As pairwise sequence identity between the $Tnp_{ISAba11}$ sequence and the 1MUS sequence is only 11%, a multistep strategy was employed to generate a satisfactory target-template alignment. First, multiple-sequence alignments for both Tn*5* and $Tnp_{ISAba11}$ homologs were generated by a series of BLAST searches, followed by sequence retrieval, alignment, and manual editing in Jalview (39). The target-template alignment was then derived from a profile-profile alignment between the two multiple-sequence alignments. Secondary structure information for Tnp_{Tn5} and secondary structure prediction for $Tnp_{ISAba11}$ were also taken into account during the alignment process. The best model out of 20 was selected based on the Modeler scoring function and manual inspection (14). Taking into account the low pairwise sequence identity, the model of $Tnp_{ISAba11}$ should be considered a low-resolution model with errors in structural details expected. The PyMOL Molecular Graphics System (version 1.2r3pre; Schrödinger, LLC) was used for visualization of the $Tnp_{ISAba11}$ model.

Nucleotide sequence accession numbers. Sequence data obtained by genomic walking have been deposited in GenBank under accession numbers JN819186 to JN819201. Further details are provided in Table S5 in the supplemental material.

RESULTS

PCR-based survey of IS*Aba11* and Tn*AbaR* carriage in *Acinetobacter*. A total of 148 strains of *Acinetobacter* species originating as epidemiologically unrelated clinical isolates were screened by PCR for the presence of IS*Aba11* and Tn*AbaR* elements. A further 48 *Acinetobacter* strains with complete or near-complete genome sequences deposited in GenBank were investigated by BlastN analysis and *in silico* PCR. Collectively, 19 or more *Acinetobacter* species were investigated (Table 1). Screening for IS*Aba11* was performed with internal $tnp_{ISAba11}$-directed primers (tnp-F/

TABLE 1 Distribution of IS*Aba11* and Tn*AbaR* elements in *Acinetobacter* strains

Acinetobacter species[a]	No. of strains analyzed			
	Total[b]	IS*Aba11* positive[e]	*tniA* positive[f]	Dually positive
A. baumannii	64 + 35 = 99	7 (4)	56	2
A. baylyi/*Acinetobacter* genomospecies 11[c]	2 + 0 = 2	0 (0)	0	0
A. berezinae	2 + 0 = 2	0 (0)	0	0
A. beijerinckii	1 + 0 = 1	1 (1)	0	0
A. calcoaceticus	1 + 2 = 3	0 (0)	0	0
Acinetobacter genomospecies 13	2 + 0 = 2	1 (1)	0	0
Acinetobacter genomospecies 16	1 + 0 = 1	0 (0)	0	0
Acinetobacter genomospecies 15TU	3 + 0 = 3	3 (3)	1	1
A. gyllenbergii	1 + 0 = 1	1 (1)	0	0
A. haemolyticus	3 + 2 = 5	4 (0)	0	0
A. johnsonii	6 + 2 = 8	6 (5)	0	0
A. junii	8 + 1 = 9	8 (8)	2	2
A. lwoffii/*Acinetobacter* genomospecies 9[c]	29 + 2 = 31	28 (26)	6	6
A. nosocomialis sp. nov.	2 + 1 = 3	0 (0)	0	0
A. parvus	3 + 0 = 3	2 (2)	0	0
A. pittii sp. nov.	7 + 1 = 8	0 (0)	1	0
A. radioresistens	3 + 2 = 5	1 (1)	1	0
A. schindleri	3 + 0 = 3	1 (0)	1	1
A. ursingii	4 + 0 = 4	1 (1)	0	0
A. ursingii group[d]	3 + 0 = 3	0 (0)	1	0

[a] One hundred eighteen strains were identified to the species level by *rpoB* gene sequencing, while a further 27 of 64 *A. baumannii* strains were identified to the species level by API NE biochemical testing and $bla_{\text{OXA-51-like}}$ PCR analysis. A final three *A. lwoffii*/*Acinetobacter* genomospecies 9 strains that were *rpoB* PCR negative were identified by API NE biochemical testing alone. Species designations corresponding to the 48 sequenced genomes analyzed were as identified in the GenBank database, with the exception of the strains currently unidentified to the species level, ATCC 27244, DR1, ADP1, RUH2624, and SH024, which were identified by *in silico rpoB* sequence analysis as *A. haemolyticus*, *A. baumannii*, *A. johnsonii*, *A. nosocomialis* sp. nov., and *A. pittii* sp. nov., respectively. Full details of strains and PCR results are shown in Tables S2 and S3 in the supplemental material.

[b] The numbers of experimentally and *in-silico*-analyzed sequenced genomes (underlined values) are shown; the latter were investigated by BlastN and *in silico* PCR analyses alone. The sequenced genomes analyzed comprised the 48 complete and near-complete *Acinetobacter* genome sequences available in GenBank as of 30 September 2011, except for the *A. baumannii* ATCC 19606 and 6013150 sequences, which were excluded to avoid duplication.

[c] *rpoB* sequence analysis could not reliably differentiate between these species.

[d] The *rpoB* sequences of the six strains assigned to this group exhibited the best match but nonidentity to the *A. ursingii rpoB* sequence.

[e] Total numbers of strains harboring intact and/or partial IS*Aba11* elements are shown; values in parentheses indicate those possessing intact IS*Aba11* elements only.

[f] *tniA* is a Tn*AbaR*-specific gene.

tnp-R) and an outer primer pair (ISAba11-F/ISAba11-R) amplifying the entire element, as we had previously noted evidence of truncated IS*Aba11* elements (B. Rieck and K. Rajakumar, unpublished data) (Fig. 1A). Combining both experimental and *in-silico*-derived data, only 4 of the 99 *A. baumannii* strains (A473, AS42, ATCC 17978, ATCC 19606) were conclusively shown to possess an intact IS*Aba11* element. However, our PCR, Southern hybridization, and genomic walking analyses of an ATCC 19606 isolate obtained in 2009 from the *Salmonella* Genetic Stock Centre suggested that our clone possessed only two partial copies of IS*Aba11*, one of which was truncated by 15 bp at the IRR terminus (see below for details). Nevertheless, as an intact IS*Aba11* sequence was recently reported for *A. baumannii* ATCC 19606 we have included these latter data in Table 1 and excluded our ATCC 19606 findings to avoid duplication (15). A fifth *A. baumannii* strain (A479) harbored a remnant of IS*Aba11* that was missing 110 and 35 bp of the IRR and inverted repeat left (IRL) termini, respectively (Fig. 1B). A sixth *A. baumannii* strain (6013113) possessed an identical 35-bp deletion at the IRL alone, while the extent of the likely partial IS*Aba11* element in *A. baumannii* strain AL7 remains to be determined. However, none of the remaining 92 *A. baumannii* strains revealed evidence of IS*Aba11* carriage by either PCR assay. In contrast, IS*Aba11* was very much more prevalent in several of the non-*A. baumannii Acinetobacter* species investigated, including *A. haemolyticus* (present in 4/5 strains examined), *A. lwoffii*/*Acinetobacter* genomospecies 9 (28/31), *A. johnsonii* (6/8), and *A. junii* (8/9) (Table 1).

The PCR survey for the presence of Tn*AbaR* elements utilized primers targeting the Tn*AbaR*-specific *tniA* gene (tniAF/tniAR) (27). The first two *A. baumannii* IS*Aba11* elements identified had been found to map to the same location within Tn*AbaR* elements. However, we observed a marked discordance in the prevalence of the two elements. Fifty-six of the 99 *A. baumannii* strains were positive for *tniA* and, by inference, for a Tn*AbaR* element, suggesting an *A. baumannii* Tn*AbaR* carriage rate of ~57%, in contrast to the 7% of *A. baumannii* strains that harbored intact and/or remnant IS*Aba11* elements (Table 1). Examination of data for the non-*A. baumannii* strains also failed to reveal obvious evidence of the "colocalization" of these two elements to a common host strain and/or *Acinetobacter* species.

Locations of IS*Aba11* in selected *Acinetobacter* sp. strains. As IS*Aba11* was known to have been inserted twice within the same site on the Tn*AbaR orf1* gene (27, 31), we sought further evidence of physical linkage between *orf1* and IS*Aba11*. However, amplification across *orf1* using primers orf1-F/orf1-R in the 12 *Acinetobacter* strains testing positive for both IS*Aba11* and Tn*AbaR* revealed no other examples of an interrupted *orf1* gene (see Fig. S1A in the supplemental material). PCR-based genome walking analysis of two *A. baumannii* and six non-*A. baumannii* strains led to the localization of IS*Aba11* elements in these empirically selected,

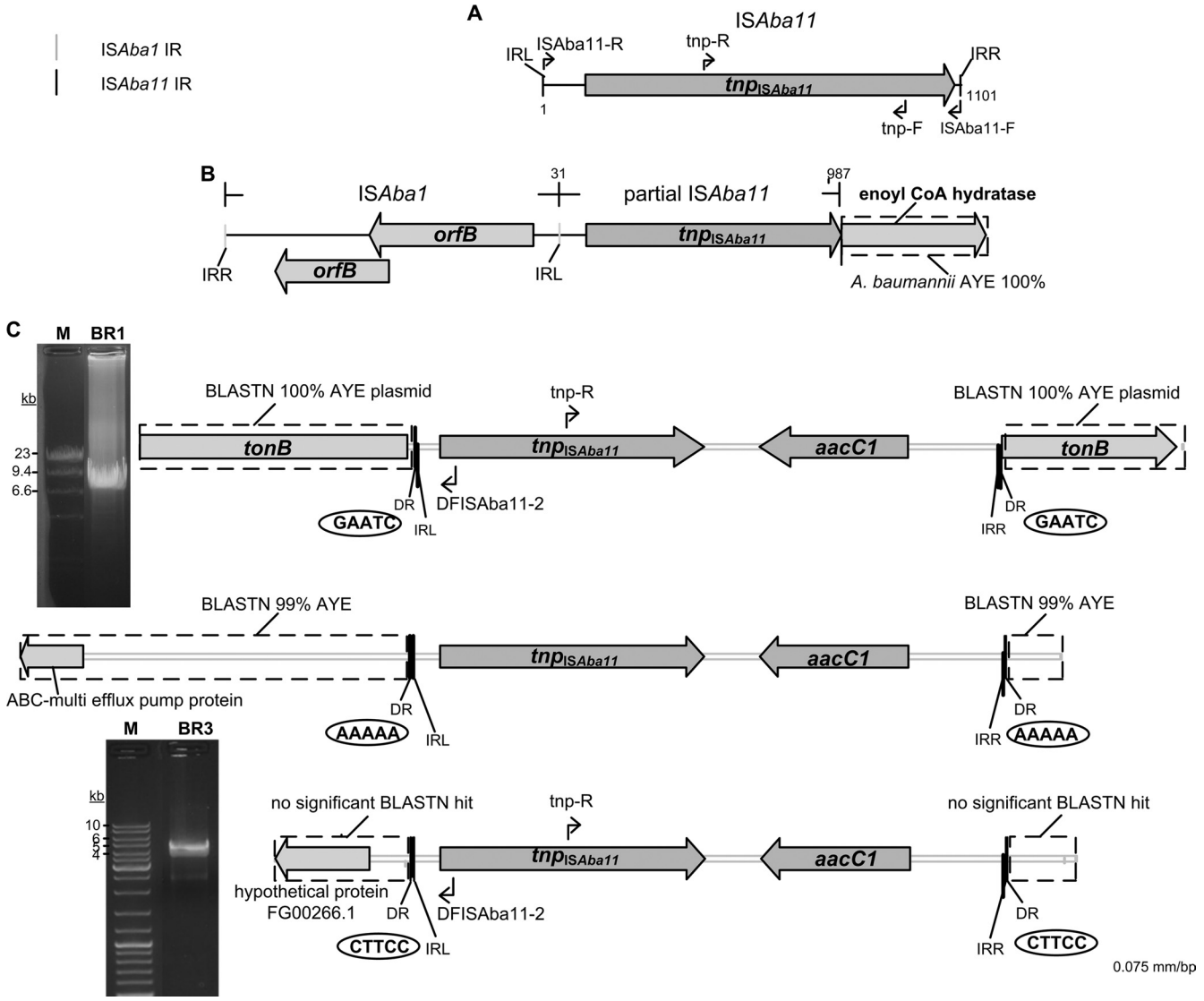

FIG 1 Locations of IS*Aba11* and IS*Aba11-aacC1* in four *A. baumannii* strains. (A) Schematic of IS*Aba11* showing locations of TIRs, primer binding sites, and $tnp_{ISAba11}$. (B) Overview of the partial IS*Aba11* element in *A. baumannii* A479 highlighting its "fusion" to an intact IS*Aba1* element. (C) Genetic contexts of IS*Aba11-aacC1* in the *A. baumannii* A424 derivatives BR1 (top), BR2 (middle), and BR3 (bottom). Identified 5-bp DRs are displayed in ellipses. Gel images show inverse-PCR amplicons (primers: DFISAba11-2/tnp-R) with BR1 (top) and BR3 (bottom) template DNA. Lane M contains a DNA molecular size ladder. Genes are shown as gray arrows and labeled with gene or protein descriptors. Numbers, where shown, are IS*Aba11* coordinates.

IS*Aba11*-positive strains. As examples, in *A. lwoffii*/*Acinetobacter* genomospecies 9 AL5 and *A. junii* AJ11, IS*Aba11* interrupted genes coding for an esterase (GenBank accession no. ZP_06069171; 98% amino acid identity) and a membrane protein (GenBank accession no. ZP_06066150; 98% amino acid identity), respectively. One of the partial copies of IS*Aba11* in our clone of *A. baumannii* ATCC 19606 was found to lie immediately downstream of a putative phospholipase C gene (GenBank accession no. EEX02177; 98% amino acid identity), and the partial copy in *A. baumannii* A479 interrupted a putative enoyl coenzyme A hydratase/isomerase gene (GenBank accession no. YP_001712458; 97% amino acid identity) and was directly "fused" to an IS*Aba1* element (Fig. 1B). The insertion site of IS*Aba11* in the incompletely assembled ATCC 19606 genome sequence could not be determined. Available insertion site data for the eight characterized strains are shown in Table S5 in the supplemental material; no duplicate target sites were detected.

Identification and characterization of *de novo* transposition of IS*Aba11* in *A. baumannii*. IS*Aba11* was tagged with an *aacC1* gentamicin resistance cassette located between the 3′ terminus of $tnp_{ISAba11}$ and the 13-bp terminal IRR. The tagged IS*Aba11* (IS*Aba11-aacC1*) sequence was introduced into the suicide vector pDS132, generating pDSISAba11Gm. This plasmid was then transferred from the *E. coli* S17.1 λ *pir*-derived donor into *A. baumannii* strain A424 by conjugation. *A. baumannii* strain A424 was chosen as the recipient because it lacked IS*Aba11* and carried a *comM*-borne Tn*AbaR* element, thus providing the opportunity to investigate whether IS*Aba11* is inserted preferentially into Tn*AbaR*. Colonies were selected by plating the overnight conjugation mixture on Simmons citrate medium supplemented with genta-

micin (80 μg/ml). Plating of donor-donor and recipient-recipient mock conjugations, as expected, led to no colonies on this medium. In contrast, each donor-recipient conjugation experiment yielded more than 300 gentamicin-resistant colonies, suggesting *de novo* IS*Aba11-aacC1* transposition or homologous recombination between the suicide plasmid and the recipient genome. Seventy randomly selected gentamicin-resistant colonies from two independent conjugation experiments were screened by PCR for *aacC1* and $tnp_{ISAba11}$ and found to be positive for both targets. However, 67 of these colonies yielded a positive band with primers aacC1R/orf1-F that amplified a 829-bp fragment spanning the *orf1*-IS*Aba11-aacC1* junction present in pDSISAba11Gm (see Fig. S1B in the supplemental material). Subsequent analysis of a further 28 independently derived gentamicin-resistant colonies suggested that few, if any, of these original 67 colonies were the result of targeted transposition of IS*Aba11-aacC1* into the A424-borne Tn*AbaR orf1* gene. Instead, the vast majority almost certainly resulted from chromosomal integration of pDSISAba11Gm following *orf1*-targeted homologous recombination between the suicide plasmid and the A424-borne *orf1* gene (see Fig. S1 in the supplemental material for details). The remaining three original colonies, representative of likely IS*Aba11-aacC1* transposition, were further characterized by genomic walking and confirmed as bearing newly transposed copies of IS*Aba11-aacC1* flanked by characteristic 5-bp DRs (Fig. 1C).

A single copy of IS*Aba11-aacC1* was mapped to a distinct genomic location in each of the three insertion mutants. In clone A424-BR1, IS*Aba11-aacC1* was inserted into a TonB-dependent receptor gene (Fig. 1C; GenBank accession no. ZP_06795313). Homologs of this gene exhibiting upwards of 98% BLASTN identity were found on eight different *A. baumannii* plasmids, including pAB0057 (8.7 kb) (1), pABVA01 (9.0 kb) (3), and pMMCU3 (9.0 kb) (GenBank accession no. GQ904227). An inverse PCR on A424-BR1 genomic DNA performed with outwardly facing IS*Aba11*-specific primers (tnp-R/DFISAba11-2) amplified an ~9.0-kb band (Fig. 1C), thus confirming that the gene targeted in A424-BR1 also lay on a similarly sized plasmid. In clone A424-BR2, IS*Aba11-aacC1* was inserted upstream of a typically chromosomally located ABC-type multidrug efflux pump gene (GenBank accession no. YP_001713963; 100% BLASTP identity) conserved in all of the *A. baumannii* strains sequenced to date (Fig. 1C). The third *de novo* IS*Aba11-aacC1* transposition event observed in A424-BR3 mapped to an entirely novel sequence that was shown to be plasmid borne by inverse PCR. The closest match, of questionable significance, was to a sequence upstream of a gene coding for a hypothetical protein in the fungus *Gibberella zeae* PH-1 (GenBank accession no. FG00266; 26% amino acid identity) (Fig. 1C). Hence, two of the three *de novo* IS*Aba11-aacC1* transposition events identified targeted plasmids rather than the chromosome.

All three characterized transposition events generated distinct but perfect 5-bp DR sequences (Fig. 1C), consistent with the IS element having targeted a different local sequence in each case and suggesting a lack of strong target sequence preference. Furthermore, examination of all of the 5-bp DR sequences associated with mapped intact iso-IS*Aba11* elements revealed insertions into at least 11 distinct target sequences (Fig. 2A). The exceptions were the previously observed targeting of a site with the same sequence within the Tn*AbaR orf1* gene and the recently reported targeting of the same site within *lpxC* in ATCC 19606 (15). If data restricted to only one end of an IS*Aba11* element were also considered, a further 12 unique insertion sites would also be recognized. The sequences TTTTT and TAAAA occur twice but in these cases correspond to IS*Aba11* insertions into distinct loci (Fig. 2A).

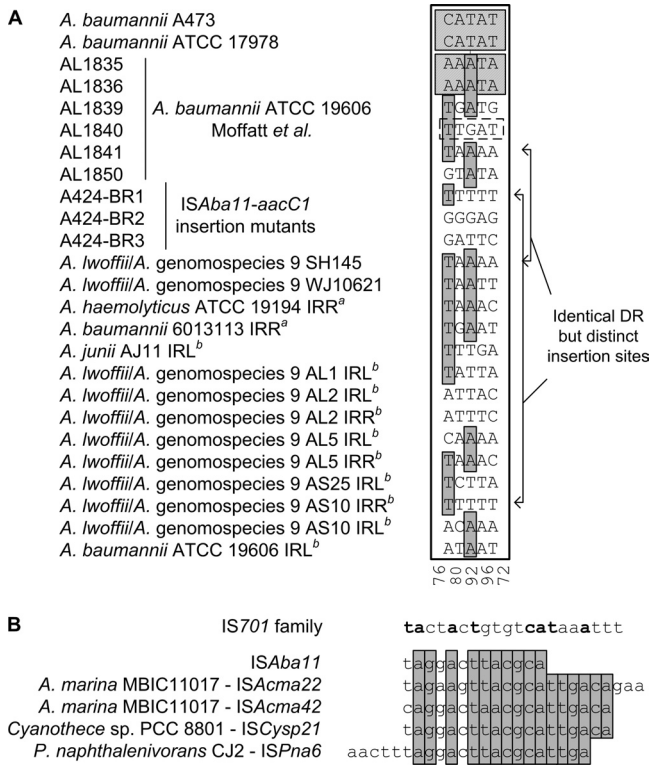

FIG 2 Repeat sequences associated with IS*Aba11* and its homologs. (A) Alignment of identified and putative 5-bp DRs flanking mapped IS*Aba11* elements. Data generated by Moffatt et al. (15) and available within the genome database are also included. The suffix IRL or IRR indicates that the data are not definitive, as flanking sequences are only available for the indicated end. The superscript letters *a* and *b* indicate a terminally truncated IS*Aba11* element and limited sequence data, respectively. Nucleotides conserved in the majority of sequences are shaded dark gray. Pairs of DRs in lighter boxes highlight identified instances of insertion at identical sites in independent strains. The DR shown in the dashed-outline box corresponds to an insertion site in *lpxC* shared by a second IS*Aba11* insertion mutant that harbors a 34-bp DR instead (15). The numbers at the bottom are the A+T percentages of the columns. (B) Alignment of IRL sequences from IS*Aba11* and its four homologs. For comparison, the consensus IS*701* family IRL, as defined by De Palmenaer et al. (6), is shown at the top (shared residues are in bold). IS*Aba11* family IRL residues that are strictly conserved are shaded gray.

IS*Aba11* copy number estimation in *Acinetobacter* species. Southern hybridization with a DIG-labeled probe specific for IS*Aba11* was performed on EcoRI-digested genomic DNA from four wild-type *A. baumannii* strains, eight non-*A. baumannii* strains, and the three newly generated IS*Aba11* insertion mutants. All were IS*Aba11* positive, except for *A. baumannii* A424. EcoRI does not cut within IS*Aba11* or *aacC1* and thus allowed the determination of minimum IS*Aba11* copy number values. This analysis showed that the IS*Aba11* copy number varied from 1 to 5 in the three natural IS*Aba11*-positive *A. baumannii* strains studied to ≥7 copies in six of the eight non-*A. baumannii* strains investigated. *A. junii* J31 possessed an estimated 13 copies (Fig. 3). As expected, no IS*Aba11*-specific band was detected for *A. baumannii* A424. Single bands were observed for A424-BR2 and A424-BR1, while the intense and smeared A424-BR3 hybridization pattern was attributed

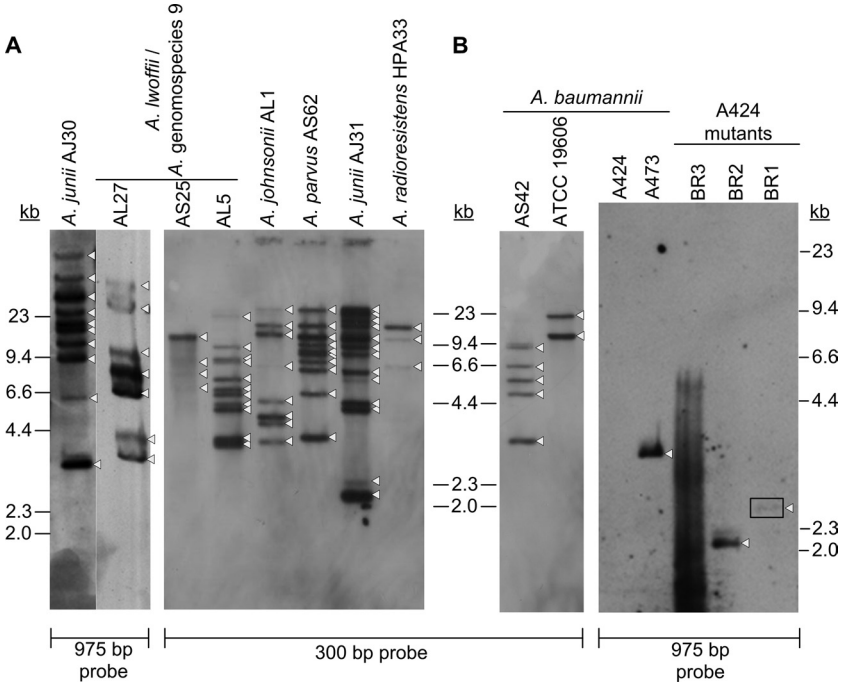

FIG 3 Southern blot-based estimation of IS*Aba11* copy numbers in selected *Acinetobacter* strains. EcoRI-digested and resolved genomic DNA from eight non-*A. baumannii* strains (A) and seven *A. baumannii* strains (B) was hybridized against a 300-bp or 975-bp IS*Aba11*-specific, DIG-labeled probe amplified from *A. baumannii* A473 genomic DNA with primers tnp-F/tnp-R and ISAba11-F/tnp-F, respectively. The positions of DNA size markers are shown. Arrowheads highlight individual detected bands, while the weak BR1-associated band is boxed.

to the ~2.5-kb IS*Aba11-aacC1*-bearing plasmid that had been identified by inverse PCR. Nevertheless, the possibility of additional IS*Aba11-aacC1* copies in A424-BR3 could not be ruled out (Fig. 3B).

***In silico* analysis of the IS*Aba11* transposase.** BLASTP analysis of $Tnp_{ISAba11}$ against the NCBI genome database revealed the presence of highly similar homologs (98 to 100% sequence identity) in nine *Acinetobacter* strains belonging to four *Acinetobacter* species, and in *Enhydrobacter aerosaccus* SK60 (Table 2). However, intact copies of iso-IS*Aba11* elements could be identified in only six strains, while variably truncated or indeterminate copies were found in the others (Table 2). Four proteins, encoded by phylogenetically distant organisms, were found to exhibit 36 to 49% identity to $Tnp_{ISAba11}$ (Fig. 4 and 5; Table 2). Genes coding for two of these resided on plasmids found in *Cyanothece* sp. strain PCC 8801 (GenBank accession no. ACK683871) and *Polaromonas naphthalenivorans* CJ2 (GenBank accession no. CP000533). Examination of flanking sequences confirmed that both mapped to typical insertion sequences (Table 2). The remaining two distant homologues, found in *Acaryochloris marina* MBIC11017, were encoded by the chromosomally borne IS*Acma22* and IS*Acma42* elements, which had been deposited in ISfinder by Swingley et al. (34).

All of the available TIR sequences for the iso-IS*Aba11* elements identified perfectly matched those of the IS*Aba11* element described in this study, while those of the four distant homologs ranged from 18 bp to 22 bp, with up to two mismatches between cognate IRL and IRR sequences. Remarkably, there was extensive identity among the IRL sequences of all five homologs (Fig. 2B). However, a characteristic flanking DR could be found for only the two elements in *A. marina* MBIC11017 and those in *Acinetobacter* spp. (Table 2), suggesting that DR generation was not necessarily a feature of these elements or that restructuring events had occurred following initial transposition.

$Tnp_{ISAba11}$ modeling based on the crystal structure of Tn*5* transposase. An InterProScan search predicts that $Tnp_{ISAba11}$ contains the "transposase DDE domain" (Pfam entry PF01609; E value, 1.4e-9), which belongs to the RNase H-like superfamily. The transposase DDE domain contains a motif of three conserved carboxylate residues (DDE), which are thought to be responsible for coordinating metal ions needed for catalysis. This has been shown conclusively in the *E. coli* Tnp_{Tn5} structure (33).

The homology model of $Tnp_{ISAba11}$ is based on the *E. coli* Tnp_{Tn5} structure (PDB entry 1MUS [33]). Tnp_{Tn5} consists of 476 amino acids, whereas $Tnp_{ISAba11}$ is only 324 amino acids long. This is attributed to significantly shorter N- and C-terminal regions and in part shorter loops between secondary structure elements in $Tnp_{ISAba11}$. For example, there are no corresponding $Tnp_{ISAba11}$ residues for the ~35 residues of the N-terminal region of Tnp_{Tn5}. Also, the 40 C-terminal $Tnp_{ISAba11}$ residues could not be aligned with the ~100 residues of the C terminus of Tnp_{Tn5} and hence were not modeled (Fig. 5C). However, a number of regions were found to be relatively conserved across the Tnp_{Tn5}-$Tnp_{ISAba11}$ profile-profile alignment. These regions are located mostly at the core of the DNA binding region, in particular, the functionally important N2, N3, and C1 regions of Tnp_{Tn5}, which include the DDE motif (D97, D188, and E326 in Tnp_{Tn5}). The DDE motif is fully conserved between Tn*5* and $Tnp_{ISAba11}$ homologs. The C1 region also contains the YREK motif (Y319, R322, E326, and K333 in Tnp_{Tn5}). The residues of the latter motif are involved

TABLE 2 Characteristic features of members of the IS*Aba11* family identified in available bacterial sequence data[a]

Strain/IS designation	Insertion sequence				Transposase	
	Length (bp)	TIR length (bp)/no. of mismatches[e]	DR length (bp)	BLASTN hit (%)[b]	No. of aa	BLASTP hit (%)[b]
Acinetobacter baumannii ATCC 17978/IS*Aba11*	1,101	13/0	5	100	324	100
Acinetobacter baumannii A473/IS*Aba11*	1,101	13/0	5	100	324	100
Acinetobacter baumannii ATCC 19606/iso-IS*Aba11*[f]	1,101	13/0	NA	99	324	98
Acinetobacter lwoffii/*Acinetobacter* genomospecies 9 SH145/iso-IS*Aba11*	1,101	13/0	5	95[c]	324	100
Acinetobacter lwoffii/*Acinetobacter* genomospecies 9 WJ10621/iso-IS*Aba11*	1,101	13/0	5	99	324	100
Enhydrobacter aerosaccus SK60/IS*Enae1*	1,101	13/0	None	98	324	100
Acinetobacter haemolyticus ATCC 27244/iso-IS*Aba11*[c]	≥1,062	13/NA	NA	98	324	99
Acinetobacter johnsonii SH046/iso-IS*Aba1*[c]	≥833	13/NA	NA	98	≥241	100
Acinetobacter baumannii 6013113/iso-IS*Aba11*[d]	1,066	13/NA	NA	98	324	98
Acinetobacter haemolyticus ATCC 19194/iso-IS*Aba11*[d]	557	13/NA	NA	98	185	100
Acaryochloris marina MBIC11017/IS*Acma22*	1,251	22/2	5	NS	350	45
Acaryochloris marina MBIC11017/IS*Acma42*	1,140	18/1	5	NS	308	36
Polaromonas naphthalenivorans CJ2(pPNAP04)/IS*Pna6*	1,134	22/1	None	NS	326	49
Cyanothece sp. strain PCC 8801(pP880101)/IS*Cysp21*	1,139	19/0	None	NS	321	44

[a] Abbreviations: aa, amino acids; NA, not available (due to incomplete sequence data and/or IS truncation); NS, not significant.
[b] BLASTN and BLASTP results are shown as percentages of identity to the IS*Aba11* and $Tnp_{ISAba11}$ sequences, respectively.
[c] Incomplete and/or poor-quality sequence data.
[d] Truncated copy of iso-IS*Aba11*.
[e] Number of mismatches between the left and right TIRs.
[f] The sequence of an intact iso-IS*Aba11* element in *A. baumannii* ATCC 19606 was recently reported by Moffatt et al. (15).

in metal coordination (E326) and DNA binding (Y319, R322, and K333) (11). A variation of the YREK motif, HHEK, was found to be conserved across all five $Tnp_{ISAba11}$ homologs shown in Fig. 4. Furthermore, the N-terminal domain showed sequence conservation between Tnp_{Tn5} and the $Tnp_{ISAba11}$ homologs in a region required for initial DNA recognition by Tnp_{Tn5} (4). This region includes R62 (corresponding to R25 in $Tnp_{ISAba11}$), which is critical for Tnp_{Tn5}-DNA interactions (37)

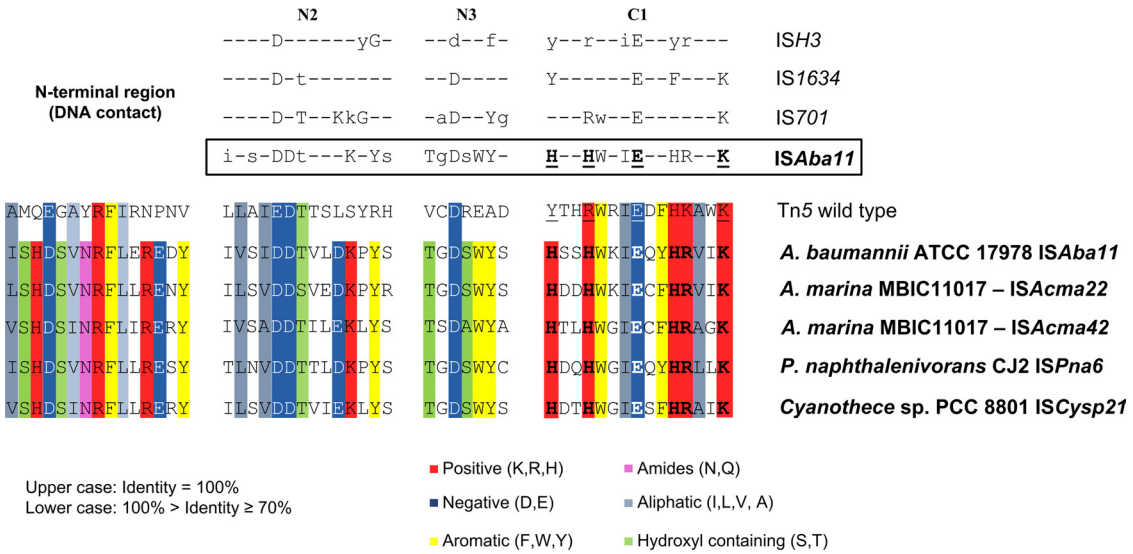

FIG 4 Alignment of key regions of $Tnp_{ISAba11}$, the four HHEK-bearing $Tnp_{ISAba11}$ homologs, and Tnp_{Tn5}. The N2, N3, and C1 regions bear the archetypal DDE residues common to many transposases. The N-terminal region is also shown, as it is highly conserved and known to partake in DNA contact during Tn*5* transposition. Tnp_{Tn5} is included as a representative IS*4* family transposase. The YREK motif of Tnp_{Tn5} (underlined residues), found in the C1 region, characterizes all of the IS*4* family transposases. The glutamic acid residue is shared between the DDE and YREK motifs. Residues within the N2, N3, and C1 regions shared by members of the IS*H3*, IS*1634*, and IS*701* families, as identified by De Palmenaer et al. (6), are shown in uppercase (strictly conserved) or lowercase (highly conserved) letters (upper panel), as appropriate. Residues shared by members of the IS*Aba11* family are similarly highlighted. The HHEK motif, which is characteristic of the IS*Aba11* family, is shown in bold and underlined. Colors indicate conserved residues with shared physiochemical properties, as depicted in the key. This figure has been adapted from a schematic first presented by De Palmenaer et al. (6).

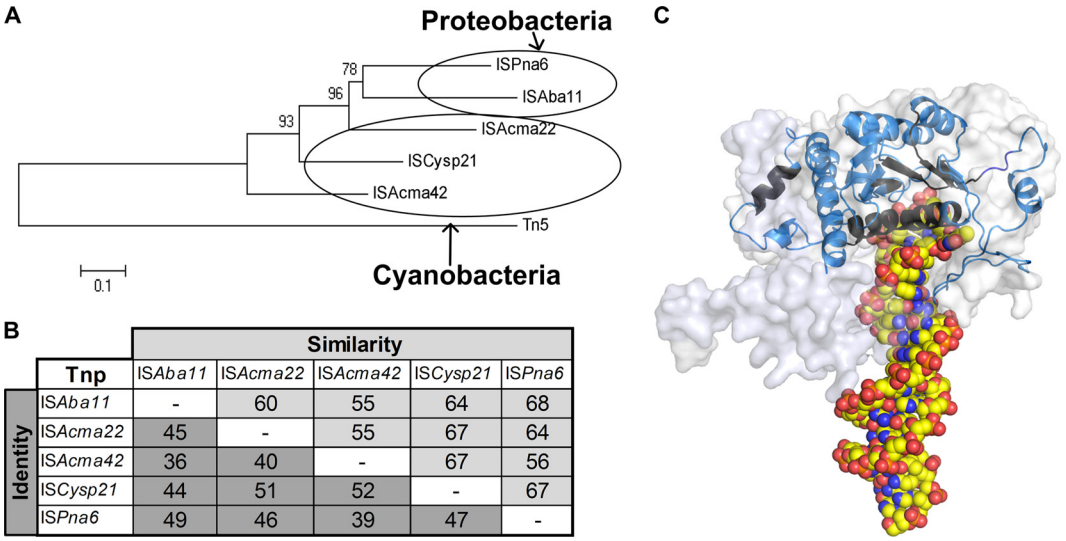

B

	Tnp	ISAba11	ISAcma22	ISAcma42	ISCysp21	ISPna6
		Similarity				
Identity	ISAba11	-	60	55	64	68
	ISAcma22	45	-	55	67	64
	ISAcma42	36	40	-	67	56
	ISCysp21	44	51	52	-	67
	ISPna6	49	46	39	47	-

FIG 5 Phylogeny, predicted structure, and similarities of $Tnp_{ISAba11}$. (A) Phylogenetic relationships of IS*Aba11* family transposases and Tnp_{Tn5}. The phylogenetic tree was generated in Mega5 (35) using the maximum-likelihood method with default settings based on the underlying profile-profile alignment between the Tn*5* and the $Tnp_{ISAba11}$ homologs as described in Materials and Methods. Ovals indicate the two associated host phyla. (B) Pairwise amino acid sequence similarity/identity matrix for $Tnp_{ISAba11}$ and its four homologs encoded by IS*Acma22*, IS*Acma42*, IS*Cysp21*, and IS*Pna6*. (C) Low-resolution homology model of the $Tnp_{ISAba11}$ monomer shown in a cartoon representation (α-helices as helices, β-strands as arrows). Color is used to indicate conservation. The most-conserved regions used for anchoring the $Tnp_{ISAba11}$-Tnp_{Tn5} alignment are highlighted in black in the $Tnp_{ISAba11}$ model ($Tnp_{ISAba11}$ residues: His20-Leu27, Ile51-Thr57, Phe135-Tyr142, Gly155-Asp163, and Phe224-Val247), while other regions of the $Tnp_{ISAba11}$ model are shown in blue. For size comparison, the overall shape of the experimentally determined Tnp_{Tn5} monomer structure (PDB entry 1MUS) is shown as a transparent surface representation. A generic DNA substrate (sphere model) is overlaid.

and is fully conserved across the entire $Tnp_{ISAba11}$ protein alignment (Fig. 4).

DISCUSSION

A. baumannii exhibited the highest Tn*AbaR* carriage rate (56/99; 57%) but a much lower IS*Aba11* positivity ranking (7%; ranked 12/19) among the species studied. In contrast, 90% of the 31 *A. lwoffii*/*Acinetobacter* genomospecies 9 strains analyzed were IS*Aba11* positive but only 19% harbored Tn*AbaR* elements. The limited Southern data also suggest that IS*Aba11* is typically found at a lower copy number in *A. baumannii* than in selected non-*A. baumannii* species. Species-specific niches may partly explain the seemingly distinct distributions of IS*Aba11* and Tn*AbaR*. For example, the vast majority of *Acinetobacter* clinical isolates are *A. baumannii* (36), a species rarely isolated from other environments. In contrast, many other *Acinetobacter* species are found primarily in soil, water, and/or inanimate environments (7), potentially hampering horizontal gene transfer between environmental and human-resident *Acinetobacter* species (5).

The presence of IS*Aba11* at the same location within the Tn*AbaR*-borne *orf1* gene in two *A. baumannii* strains could reflect divergence from a common clone or independent IS*Aba11* insertion events. As Tn*AbaR* has been hypothesized to transpose via a Tn*7*-analogous mechanism, Orf1 would be predicted to be essential for transposition. Hence, a cut-and-paste Tn*AbaR* element carrying an IS*Aba11*-disrupted *orf1* gene would be stabilized, as with the role of IS*26* in locking-in the $bla_{CTX\text{-}M}$-laden IS*Ecp* element (40). Moffatt et al. have recently shown that IS*Aba11* can target two lipid A biosynthesis pathway genes (*lpxA*, *lpxC*). Eight such mutants were identified in their study. Two each carried IS*Aba11* elements that had targeted distinct sites with the same sequences in *lpxC*, suggesting the presence of insertion hot spots within this gene (15). Nonetheless, available data suggest that IS*Aba11* displays target promiscuity, as we have identified 23 distinct definite or likely insertion sites, suggesting, at best, low-level targeting of the Tn*AbaR orf1* and *lpxC* genes and a possible slight bias toward A+T-rich loci (Fig. 2A).

The low pairwise identity values (36 to 52%) among the five HHEK-bearing $Tnp_{ISAba11}$ homologs suggest that these proteins and, by extension, the associated IS elements have evolved from a common ancestor that existed in the distant past (Fig. 5A). Horizontal gene transfer between phylogenetically distant species is thought to be rare, and IS dissemination of this nature typically reflects ancient transposition and subsequent evolutionary divergence (38). Transphylum and even transdomain distribution of members of an IS family has been reported. Cassier-Chauvat et al. identified an IS element found in the cyanobacterium *Synechocystis* which had a significant homolog in alphaproteobacteria (2), while the *Shigella dysenteriae* IS*1* transposase exhibits amino acid identity of up to 48% with IS-encoded transposases in archaea (20). In contrast, copies of IS elements in closely related species often approach identity, reflecting very recent dissemination. This is the case for the iso-IS*Aba11* elements identified in *Acinetobacter* spp. and the single *E. aerosaccus* representative, consistent with both *Acinetobacter* and *Enhydrobacter* belonging to the *Moraxellaceae* family of the class *Gammaproteobacteria*. The restricted distribution and low copy number of IS*Aba11* in *A. baumannii*, as opposed to its frequent and abundant presence in other selected *Acinetobacter* species, suggest that IS*Aba11* has only recently entered the *A. baumannii* gene pool, most probably via direct transfer from another *Acinetobacter* species. Assuming that IS*Aba11* behaves as a cut-and-paste element, like its IS*4* relatives, copy

number expansion would require repeated horizontal acquisition and/or entry on a multicopy plasmid (Table 1).

Three distinct variations of the archetypal IS*4* transposase family YREK motif had been previously identified by De Palmenaer et al. (6), leading these authors to regroup IS elements with these motifs into the independent IS families, IS*701*, IS*H3*, and IS*1634*. IS*Aba11* had been posted on ISfinder as a member of the IS*701* family (31). However, identification of the novel HHEK motif in $Tnp_{ISAba11}$ and its homologs; high-level conservation of cognate TIRs; and recognition that insertion of IS*Aba11*, IS*Acma22*, and IS*Acma42* generates a 5-bp DR instead of the 4-bp DR typical of IS*701* family members (6) led us to assign IS*Aba11* and its homologs to a new family designated the IS*Aba11* family. Indeed, based on differences in DR and TIR lengths and the extent of nucleotide conservation between IS*Aba11* and members of the IS*701* and IS*4* families, Moffatt et al. had also recently proposed that IS*Aba11* be assigned to a new IS family (15). Notably, the single representatives of IS*Cysp21* and IS*Pna6* and the only identified non-*Acinetobacter*-borne iso-IS*Aba11* element were not associated with flanking DRs (Table 2). Additionally, Moffatt et al. had reported a single instance of a newly transposed IS*Aba11* element being flanked by 34-bp perfect DRs (15), suggesting the possibility of low-frequency alternate cleavage sites during IS*Aba11* transposition (22). A further 22 IS elements present in seven bacterial phyla and one archaeal phylum encode transposases with marked similarity to $Tnp_{ISAba11}$. Remarkably, these elements possess TIRs resembling those of the IS*Aba11* family, but none encodes a transposase with a complete HHEK motif, raising the possibility of broadening the IS*Aba11* family to include elements with the less stringent HEK or EK submotif as well (see Fig. S2 in the supplemental material).

The five HHEK-bearing IS*Aba11* family transposases share significant sequence similarity with the Tnp_{Tn5} DDE domain that is known to bind to DNA during transposition; in particular, the DDE motif is fully conserved (33). This suggests that IS*Aba11* family transposases could utilize a similar method of TIR sequence recognition to that of Tnp_{Tn5} (33). However, a variety of distinctive features between IS*Aba11* family and Tn*5* transposases suggests divergence of the DNA sequence recognition process. Indeed, the contrasting lengths of the 19-bp Tn*5* TIR and the 13-bp IS*Aba11* TIR appear to correspond to the different sizes of the DNA binding domains in Tnp_{Tn5} and $Tnp_{ISAba11}$, the latter having been predicted by the three-dimensional modeling performed in this study. $Tnp_{ISAba11}$ appears to be a "minimal" version of Tnp_{Tn5}, consistent with the reduced protein-DNA interaction space associated with the shorter IS*Aba11* TIRs. Secondary structure predictions of $Tnp_{ISAba11}$ also suggest the presence of a C-terminal α-helix, which is not included in the $Tnp_{ISAba11}$ model, as this region could not be reliably aligned with Tnp_{Tn5}. The equivalent region in Tnp_{Tn5} forms an α-helical subdomain which has been shown to mediate protein-protein interactions (33). Analogously, the predicted C-terminal α-helix of $Tnp_{ISAba11}$ may well be involved in dimerization.

The precise mechanisms of IS*Aba11* transposition, factors that govern transposition efficiency, barriers to wider taxonomic dissemination, and the potential impact of this element on the downstream evolution of *Acinetobacter* warrant further study. The recent report of IS*Aba11*-mediated colistin resistance is clearly of major concern (15). Indeed, should IS*Aba11* permeate *A. baumannii* as it has done in a number of other *Acinetobacter* species, widespread resistance to this last-resort agent may become a feature of endemic *A. baumannii* strains.

ACKNOWLEDGMENTS

We thank Owen Lancaster for help with bioinformatics, Donna Mathew for technical assistance, and Jon van Aartsen for helpful advice. Major thanks to Te-Li Chen (Division of Infectious Diseases, Taipei Veterans General Hospital, Taipei, Taiwan, Republic of China), Simon Hewson, Eva Horvath-Papp, and Kevin Towner for providing *Acinetobacter* strains.

This work was funded by a BSAC grant to K.R.

REFERENCES

1. **Adams MD, et al.** 2008. Comparative genome sequence analysis of multidrug-resistant *Acinetobacter baumannii*. J. Bacteriol. **190**: 8053–8064.
2. **Cassier-Chauvat C, Poncelet M, Chauvat F.** 1997. Three insertion sequences from the cyanobacterium *Synechocystis* PCC6803 support the occurrence of horizontal DNA transfer among bacteria. Gene **195**:257–266.
3. **D'Andrea MM, et al.** 2009. Characterization of pABVA01, a plasmid encoding the OXA-24 carbapenemase from Italian isolates of *Acinetobacter baumannii*. Antimicrob. Agents Chemother. **53**:3528–3533.
4. **Davies DR, Goryshin IY, Reznikoff WS, Rayment I.** 2000. Three-dimensional structure of the Tn*5* synaptic complex transposition intermediate. Science **289**:77–85.
5. **de la Cruz F, Davies J.** 2000. Horizontal gene transfer and the origin of species: lessons from bacteria. Trends Microbiol. **8**:128–133.
6. **De Palmenaer D, Siguier P, Mahillon J.** 2008. IS*4* family goes genomic. BMC Evol. Biol. **8**:18.
7. **Doughari HJ, Ndakidemi PA, Human IS, Benade S.** 2011. The ecology, biology and pathogenesis of *Acinetobacter* spp.: an overview. Microbes Environ. **26**:101–112.
8. **Fournier PE, et al.** 2006. Comparative genomics of multidrug resistance in *Acinetobacter baumannii*. PLoS Genet. **2**:e7.
9. **Hallet B, Rezsohazy R, Mahillon J, Delcour J.** 1994. IS*231A* insertion specificity: consensus sequence and DNA bending at the target site. Mol. Microbiol. **14**:131–139.
10. **Kennedy AK, Guhathakurta A, Kleckner N, Haniford DB.** 1998. Tn*10* transposition via a DNA hairpin intermediate. Cell **95**:125–134.
11. **Klenchin VA, et al.** 2008. Phosphate coordination and movement of DNA in the Tn*5* synaptic complex: role of the (R)YREK motif. Nucleic Acids Res. **36**:5855–5862.
12. **Krizova L, Dijkshoorn L, Nemec A.** 2011. Diversity and evolution of AbaR genomic resistance islands in *Acinetobacter baumannii* strains of European clone I. Antimicrob. Agents Chemother. **55**:3201–3206.
13. **Mahillon J, Chandler M.** 1998. Insertion sequences. Microbiol. Mol. Biol. Rev. **62**:725–774.
14. **Martí-Renom MA, et al.** 2000. Comparative protein structure modeling of genes and genomes. Annu. Rev. Biophys. Biomol. Struct. **29**:291–325.
15. **Moffatt J, et al.** 2011. The insertion sequence IS*Aba11* is involved in colistin resistance and loss of lipopolysaccharide in *Acinetobacter baumannii*. Antimicrob. Agents Chemother. **55**:3022–3024.
16. **Mugnier PD, Poirel L, Nordmann P.** 2009. Functional analysis of insertion sequence IS*Aba1*, responsible for genomic plasticity of *Acinetobacter baumannii*. J. Bacteriol. **191**:2414–2418.
17. **Mussi MA, Limansky AS, Viale AM.** 2005. Acquisition of resistance to carbapenems in multidrug-resistant clinical strains of *Acinetobacter baumannii*: natural insertional inactivation of a gene encoding a member of a novel family of beta-barrel outer membrane proteins. Antimicrob. Agents Chemother. **49**:1432–1440.
18. **Nagai T, Phan Tran LS, Inatsu Y, Itoh Y.** 2000. A new IS*4* family insertion sequence, IS*4Bsu1*, responsible for genetic instability of poly-gamma-glutamic acid production in *Bacillus subtilis*. J. Bacteriol. **182**: 2387–2392.
19. **Ochman H, Gerber AS, Hartl DL.** 1988. Genetic applications of an inverse polymerase chain reaction. Genetics **120**:621–623.
20. **Ohta S, et al.** 2002. Presence of a characteristic D-D-E motif in IS*1* transposase. J. Bacteriol. **184**:6146–6154.
21. **Pilhofer M, et al.** 2007. Characterization of bacterial operons consisting of two tubulins and a kinesin-like gene by the novel two-step gene walking method. Nucleic Acids Res. **35**:e135.
22. **Plikaytis BB, Crawford JT, Shinnick TM.** 1998. IS*1549* from *Mycobac-*

terium smegmatis forms long direct repeats upon insertion. J. Bacteriol. **180**:1037–1043.
23. **Poirel L, et al.** 2005. OXA-58, a novel class D {beta}-lactamase involved in resistance to carbapenems in *Acinetobacter baumannii*. Antimicrob. Agents Chemother. **49**:202–208.
24. **Poirel L, Nordmann P.** 2006. Genetic structures at the origin of acquisition and expression of the carbapenem-hydrolyzing oxacillinase gene *bla*OXA-58 in *Acinetobacter baumannii*. Antimicrob. Agents Chemother. **50**:1442–1448.
25. **Quevillon E, et al.** 2005. InterProScan: protein domains identifier. Nucleic Acids Res. **33**:W116–W120.
26. **Reznikoff WS.** 2008. Transposon Tn*5*. Annu. Rev. Genet. **42**:269–286.
27. **Rose A.** 2010. Tn*AbaR1*: a novel Tn*7*-related transposon in *Acinetobacter baumannii* that contributes to the accumulation and dissemination of large repertoires of resistance genes. Biosci. Horiz. **3**:40–48.
28. **Sambrook J, Fritsch EF, Maniatis T.** 1989. Molecular cloning: a laboratory manual, 2nd ed. Cold Spring Harbor Laboratory Press, Cold Spring Harbor, NY.
29. **Siguier P, Filee J, Chandler M.** 2006. Insertion sequences in prokaryotic genomes. Curr. Opin. Microbiol. **9**:526–531.
30. **Siguier P, Perochon J, Lestrade L, Mahillon J, Chandler M.** 2006. ISfinder: the reference centre for bacterial insertion sequences. Nucleic Acids Res. **34**:D32–D36.
31. **Smith MG, et al.** 2007. New insights into *Acinetobacter baumannii* pathogenesis revealed by high-density pyrosequencing and transposon mutagenesis. Genes Dev. **21**:601–614.
32. **Söding J.** 2005. Protein homology detection by HMM-HMM comparison. Bioinformatics **21**:951–960.
33. **Steiniger-White M, Rayment I, Reznikoff WS.** 2004. Structure/function insights into Tn*5* transposition. Curr. Opin. Struct. Biol. **14**:50–57.
34. **Swingley WD, et al.** 2008. Niche adaptation and genome expansion in the chlorophyll d-producing cyanobacterium *Acaryochloris marina*. Proc. Natl. Acad. Sci. U. S. A. **105**:2005–2010.
35. **Tamura K, et al.** 2011. MEGA5: molecular evolutionary genetics analysis using maximum likelihood, evolutionary distance, and maximum parsimony methods. Mol. Biol. Evol. **28**:2731–2739.
36. **Turton JF, Shah J, Ozongwu C, Pike R.** 2010. Incidence of *Acinetobacter* species other than *A. baumannii* among clinical isolates of *Acinetobacter*: evidence for emerging species. J. Clin. Microbiol. **48**:1445–1449.
37. **Twining SS, Goryshin IY, Bhasin A, Reznikoff WS.** 2001. Functional characterization of arginine 30, lysine 40, and arginine 62 in Tn*5* transposase. J. Biol. Chem. **276**:23135–23143.
38. **Wagner A, de la Chaux N.** 2008. Distant horizontal gene transfer is rare for multiple families of prokaryotic insertion sequences. Mol. Genet. Genomics **280**:397–408.
39. **Waterhouse AM, Procter JB, Martin DM, Clamp M, Barton GJ.** 2009. Jalview version 2—a multiple-sequence alignment editor and analysis workbench. Bioinformatics **25**:1189–1191.
40. **Zong Z, Partridge SR, Iredell JR.** 2010. IS*Ecp1*-mediated transposition and homologous recombination can explain the context of *bla*(CTX-M-62) linked to *qnrB2*. Antimicrob. Agents Chemother. **54**:3039–3042.